ELSEVIER

Biochimica et Biophysica Acta 1290 (1996) 241–249

BBA Biochimica et Biophysica Acta

Identity of zinc ion-dependent acid phosphatase from bovine brain and *myo*-inositol 1-phosphatase

Anna Caselli [a], Paolo Cirri [a], Stefania Bonifacio [a], Giampaolo Manao [a], Guido Camici [a], Gianni Cappugi [a], Gloriano Moneti [b], Giampietro Ramponi [a,*]

[a] *Dipartimento di Scienze Biochimiche, Università di Firenze, Viale Morgagni 50, I-50134 Firenze, Italia*
[b] *Dipartimento di Farmacologia Preclinica e Clinica, Università di Firenze, Viale Morgagni 65, I-50134 Firenze, Italia*

Received 18 January 1996; accepted 14 February 1996

Abstract

A 62 kDa Zn^{2+}-dependent acid phosphatase has been purified from bovine brain. The protein was carboxymethylated and then cleaved by endoproteinase Glu-C, trypsin and CNBr. Several fragments were subjected to structural analysis either by using mass spectrometry or automated peptide sequencing. The four sequenced peptides were compared with the known protein sequences contained in the EMBL Data Bank. All four peptide sequences were identical to the corresponding amino-acid sequences present in *myo*-inositol 1-phosphatase from bovine brain. Furthermore we found that the amino-acid composition of Zn^{2+}-dependent acid phosphatase purified in our laboratory is very similar to that of *myo*-inositol 1-phosphatase, and that several peptide fragments have molecular weights (measured by mass spectrometry techniques) identical to those expected for cleavage-fragments originated from the authentic *myo*-inositol 1-phosphatase. This is one of the key enzymes in the receptor-stimulated inositol phospholipid metabolism and it has been considered as the probable target of Li^+ ion during LiCl therapy in manic-depressive patients. The comparison of the Zn^{2+}-dependent acid phosphatase and the Mg^{2+}-dependent *myo*-inositol-1-phosphatase activities, measured at different purification steps, shows that the ratio between the two activities was remarkably constant during enzyme purification. We also demonstrated that in the presence of Mg^{2+} this enzyme efficiently catalyses the hydrolysis of *myo*-inositol 1-phosphate, and that the Li^+ ion inhibits this activity. Furthermore, the thermal treatment of the enzyme causes a time-dependent parallel decrease of both Zn-dependent *p*-nitrophenyl phosphatase (assayed at pH 5.5) and Mg^{2+}-dependent *myo*-inositol-1-phosphatase (assayed at pH 8.0) activities, suggesting the hypothesis that the same protein possesses both these activities.

Keywords: Zinc ion-dependent acid phosphatase; *myo*-Inositol 1-phosphatase; Phosphatase; (Bovine brain)

1. Introduction

The different phosphomonohydrolases present in biological systems have different catalytic strategies [1]. Some catalytic mechanisms are common to enzymes that act on specific phosphorylated substrates. This is the case of phosphotyrosine protein phosphatases that control the levels of tyrosine phosphorylated proteins involved in mitogenic signalling and other processes. All phosphotyrosine protein phosphatases form a covalent thiol-phosphate intermediate during catalysis [2]. Also non-specific phosphatases, such as alkaline and the true acid phosphatases (i.e., those of lysosomal and bacterial origin), form covalent phospho-enzyme intermediate during catalysis; alkaline phosphatases form *O*-phospho-serine, and acid phosphatases form *N*-phosphohistidine [1]. The phosphoserine/phosphothreonine protein phosphatases do not form covalent enzyme-phosphate intermediates during their catalytic processes.

Acid phosphatases (EC 3.1.3.2) are generally classified as non-specific enzymes and often occur in multiple molecular forms [3]. They differ in molecular size and cellular localisation, as well as in substrate specificity and

Abbreviations: PMSF, phenylmethanesulfonyl fluoride; Cm, carboxymethyl; MS, mass spectrometry; MALDI, matrix-assisted laser-desorption ionisation; TOF, time-of-flight; ES, ion spray; PVDF, polyvinylidene difluoride; TFA, trifluoroacetic acid; *myo*-IP, D-*myo*-inositol 1-phosphate; PNPP, *p*-nitrophenylphosphate; sp, endoproteinase Glu-C peptide; SDS, sodium dodecyl sulfate; PAGE, polyacrylamide gel electrophoresis.

* Corresponding author. Fax: +39 55 4222725; e-mail: dpt-bioch@cesit1.unifi.it.

PII S0304-4165(96)00022-0

susceptibility to inhibitors. There is also a particular class of acid phosphatases that require metal ions for activity [4–7]. The Zn^{2+}-dependent acid phosphatase has been detected in several animal tissues and species [7]; two main molecular forms, differing in tissue distribution, have been found. Brain, heart, skeletal muscle, erythrocytes, lung, spleen, and stomach contain a 62 kDa molecular form of the Zn^{2+}-dependent acid phosphatase, whereas liver contains a higher molecular weight form of the enzyme. The small intestine and kidney contain both high and low molecular weight forms [7]. Fujimoto et al. [7] purified the bovine brain low molecular weight form and found that the enzyme is a dimeric protein. Vesicles containing millimolar concentrations of the zinc ion have been detected in particular brain structures (Fraústo da Silva and Williams [8]). These authors suggested that these particular zinc stores, like those of calcium, are the results of special zinc ion pump activity, and may be involved in signalling processes. Since phosphatases are involved in the balancing of the kinase activity in several signalling processes, we think that it is important to enhance the information on the zinc-dependent acid phosphatase from the bovine brain. This paper reports a new purification procedure of the zinc-dependent acid phosphatase and a study on its molecular properties. Surprisingly, structural and kinetic studies on this enzyme preparation reveal that the zinc-dependent acid phosphatase and *myo*-inositol 1-phosphatase are present in the same protein.

2. Materials and methods

Bovine brain was purchased from the local slaughterhouse. D-*myo*-Inositol 1-phosphate, *p*-nitrophenyl phosphate, and L-phosphotyrosine were obtained from Sigma. SP-Trisacryl (LKB) and Superdex-200 columns were purchased from Pharmacia. HPLC columns: Bio-Sil PEG 300-10 (10 × 150 mm) was from Bio-Rad; Protein and Peptide C18 (4.6 × 250 mm) was from Vydac. All other reagents were the purest commercially available.

2.1. Purification of the Zn^{2+}-dependent acid phosphatase

Step 1. Bovine brain (2 kg) was minced and homogenised in a Waring blender with 3 vols. of 0.05 M sodium acetate buffer (pH 5.5), containing 1 mM EDTA, 2 mM 2-mercaptoethanol, and 0.1 mM PMSF. The homogenate was stirred for 90 min, and then centrifuged at 7000 × *g* for 50 min. The precipitate was discarded.

Step 2. Ammonium sulfate was slowly added to the supernatant (40% saturation). The precipitate was discarded, and ammonium sulfate (80% saturation) was added in order to precipitate the enzyme. After standing for 30 min, the precipitate was collected by centrifugation at 15 000 × *g* for 30 min, dissolved in 700 ml of 0.025 M Tris-HCl buffer (pH 7.0), containing 1 mM EDTA, 2 mM 2-mercaptoethanol and 0.1 mM PMSF, and then dialysed against the same buffer.

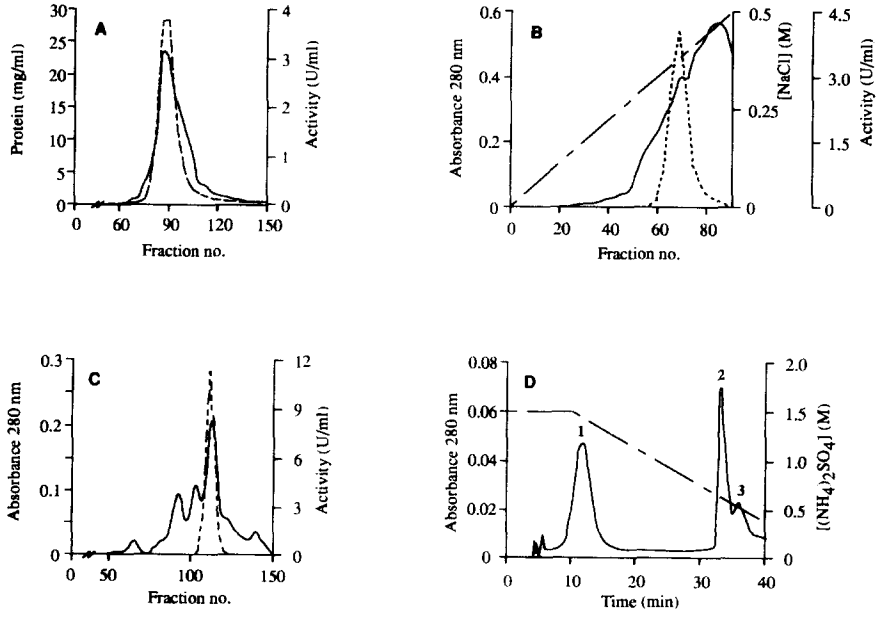

Fig. 1. (A) DEAE-cellulose chromatography. The column (8 × 45 cm) was eluted with 0.025 M Tris-HCl buffer (pH 7.0) containing 1 mM EDTA, 2 mM 2-mercaptoethanol, 0.1 mM PMSF and 0.4 M NaCl at a flow rate of 120 ml/h and 20 ml fractions were collected. (B) SP-trisacryl chromatography. The column (2.6 × 50 cm) was eluted with a linear NaCl gradient in 50 mM sodium acetate buffer (pH 4.5) containing 1 mM EDTA and 2 mM 2-mercaptoethanol, at a flow rate of 60 ml/h and 10 ml fractions were collected. (C) Superdex 200 chromatography. The column (2.6 × 60 cm) was eluted with 0.025 M Tris-HCl buffer (pH 7.0) containing 1 mM EDTA and 2 mM 2-mercaptoethanol, at a flow rate of 120 ml/h and 2 ml fractions were collected. (D) Bio-Sil PEG 300-10 HPLC. The column (10 × 150 mm) was equilibrated with 0.025 M Tris-HCl buffer (pH 7.0) containing 2 M ammonium sulfate and eluted with a decreasing ammonium sulfate gradient as indicated. Flow rate was 2 ml/min. Only peak 2 contains the phosphatase activity. The symbols used are: (————) protein concentration; (- - -) Zn^{2+}-dependent acid phosphatase activity; (– · –) salt gradient.

Step 3. The precipitate formed during dialysis was discarded by centrifugation, and the supernatant was applied to a DEAE-cellulose column (8 × 45 cm) equilibrated with the dialysis buffer. The column was washed with 2 volumes of the same buffer, and the proteins were eluted with 0.4 M NaCl. Fig. 1A reports the elution profile of the DEAE-cellulose chromatography. The active fractions were pooled and the enzyme was precipitated by adding 70% saturation ammonium sulfate.

Step 4. The above precipitate was collected by centrifugation at 15000 × *g* for 40 min, dissolved in 100 ml of 25 mM Tris-HCl buffer (pH 7.0) containing 1 mM EDTA, 2 mM 2-mercaptoethanol, 0.1 mM PMSF and then dialysed against 100 vols. of 50 mM sodium acetate buffer (pH 4.5) containing 1 mM EDTA, 2 mM 2-mercaptoethanol, and 0.1 mM PMSF. Foreign proteins precipitated during dialysis were discarded by centrifugation, thus increasing the specific activity.

Step 5. The supernatant was applied to a cation exchange column (SP-Trisacryl, 2.6 × 50 cm) previously equilibrated with 50 mM sodium acetate buffer (pH 4.5) containing 1 mM EDTA and 2 mM 2-mercaptoethanol. The column was washed with 7 vols. of the same buffer, and the proteins were eluted by a salt gradient (from 0 to 0.5 M NaCl dissolved in the same buffer). Fig. 1B reports the elution profile of SP-Trisacryl chromatography. The active fractions were pooled and the enzyme was precipitated by adding ammonium sulfate (70% saturation). The precipitate was collected by centrifugation at 20,000g, and dissolved in 15 ml of 0.025 M Tris-HCl buffer (pH 7.0), containing 1 mM EDTA and 2 mM 2-mercaptoethanol.

Step 6. The above solution (in 5 ml batches) was applied to a Superdex-200 column (2.6 × 60 cm), equilibrated with 0.025 M Tris-HCl buffer (pH 7.0) containing 1 mM EDTA and 2 mM 2-mercapto-ethanol, and then the column was eluted with the same buffer. Fig. 1C shows the elution profile. Compared with the elution volumes of the standard proteins used to calibrate the column, the enzyme activity peak was eluted at a volume that corresponds to a molecular weight of about 60000.

Step 7. The pooled active fractions were concentrated by ultrafiltration using Centricon-30 (Amicon) membranes, and then several portions were applied to a Bio-Sil PEG 300-10 HPLC column to perform hydrophobic chromatography. Fig. 1D shows the elution profile.

2.2. Polyacrylamide gel electrophoresis

SDS-PAGE was carried out by the method of Laemmli [9] with a 15% gel.

2.3. Enzyme assays

Zn^{2+}-dependent acid phosphatase activity was determined at 37°C using 2.5 mM *p*-nitrophenyl phosphate dissolved in 0.1 M Mes-NaOH buffer (pH 5.5) containing 5 mM $ZnCl_2$ in a final volume of 1 ml. The reaction was stopped by the addition of 4 ml of 0.1 M KOH. The absorbance of the released *p*-nitrophenolate was read at 400 nm using a molar absorbance coefficient of 18000 M^{-1} cm^{-1}. The unit is defined as the amount of the enzyme that catalyzes the hydrolysis of 1 μmol of substrate per min at 37°C. L-Phosphotyrosine and phenyl phosphate phosphatase activities were assayed at 37°C using L-phosphotyrosine and phenyl phosphate as substrates; they were dissolved in 0.1 M Mes-NaOH buffer (pH 5.5) containing 5 mM $ZnCl_2$, and the reaction was stopped by adding 1 ml 1 M NaOH. The phenols produced were measured spectrophotometrically using the extinction coefficients $\varepsilon_{287} = 2560$ M^{-1} cm^{-1} for phenol and $\varepsilon_{293.5} = 2330$ M^{-1} cm^{-1} for tyrosine, all in alkaline solution. The *myo*-inositol-1-phosphatase activity was determined at 37°C using 1 mM *myo*-inositol-1-phosphate as substrate dissolved in 0.04 M Tris-HCl buffer (pH 8.0) containing 2 mM $MgCl_2$ in a final volume of 0.3 ml. The reaction was stopped by adding 20 μl of 50% trichloroacetic acid and then centrifuged at 12500 × *g* for 10 min. Aliquots of the supernatant (10–20 μl) were withdrawn, diluted to 300 μl with distilled water and then 75 μl of the Malachite green reagent [10] were added in order to determine the released inorganic phosphate. A P_i calibration curve was determined by using standard solutions of potassium dihydrogenphosphate. The developed colour was read at 600 nm using an EIA reading photometer. The release of P_i from D-*myo*-inositol 1,4-bisphosphate, D-*myo*-inositol 1,4,5-triphosphate, β-glycerophosphate, 2′-AMP, and 2′-GMP was assayed by the Malachite green reagent [10], as described for *myo*-inositol 1-phosphate. The determination of K_m and V_{max} on *myo*-inositol 1-phosphate was performed by measuring the initial hydrolysis rates by the method described by Gee et al. [11]. This method was used in order to compare our apparent kinetic parameter values relative to *myo*-inositol 1-phosphate with those previously found by other authors for the authentic *myo*-inositol 1-phosphatase [11].

2.4. Protein determination

Protein concentration was determined using the BCA-1 kit (bicinchoninic acid) for protein determination (Sigma). Alternatively, the chromatographic fractions were assayed for protein concentration by reading the absorbance at 280 nm.

2.5. Enzyme cleavages

The enzyme was first carboxymethylated and then cleaved by endoproteinase Glu-C, trypsin and CNBr. The carboxymethylation and cleavages were carried out as previously described [12].

Table 1
Summary of the purification procedure starting from bovine brain (2 kg)

Step	Volume (ml)	Total protein (mg)	Total activity (μmol/min)		Activity ratio (*myo*-IPIPNPP)	Specific activity (μmol/min per mg)		Purification on PNPP factor	Yield (%) on PNPP
			on *myo*-IP	on PNPP		on *myo*-IP	on PNPP		
1. Crude extract	4500	43650	2700	810	3.30	0.06	0.02	1	100
2. $(NH_4)_2SO_4$ (40%40%)	1000	19800	193	1106	0.17	0.01	0.06	3.0	136
3. DEAE-cellulose	820	7585	186	1058	0.18	0.02	0.14	7.0	130
4. Dialysis at pH 4.5	235	2432	153	799	0.19	0.06	0.33	16.5	99
5. SP-Trisacryl	91	31.3	108	491	0.22	3.45	15.7	785	61
6. Superdex 200	1.2	8.5	47.4	200	0.23	5.58	23.5	1175	25
7. Bio-Sil PEG 300-10	1.2	2.1	24.8	139	0.18	11.8	66.2	3310	17

2.6. Peptide purification

Peptides from the endoproteinase Glu-C digestion were separated by HPLC using the Protein and Peptide C18 reverse-phase column (4.6 × 250 mm, 5 μm). The elution was performed using the solvent system and gradient as indicated in Fig. 3 legend.

2.7. Peptide sequence analysis

Amino-acid sequence analyses of some peptides obtained by proteolytic digestion were performed by using the Protein Sequencer from Milligen. First the peptides were covalently immobilised on arylamine-PVDF membranes (Sequelon-AA, Milligen) and then the sequencer runs were performed.

2.8. Mass spectrometry

The sequence assignments of tryptic fragments were performed by continuous HPLC-ion-spray mass spectrometry. Electrospray mass spectra were acquired on a Platform mass spectrometer (Fisons Instruments, Manchester, UK). The HPLC-electrospray spectra of the tryptic digest in positive ion mode were obtained under the following conditions: HPLC on the Protein and Peptide C18 column (4.6 × 250 mm, 5 μm) at a flow rate 1 ml/min; solvent A: 10 mM TFA in water; solvent B: 10 mM TFA in acetonitrile; the solvent B gradient was as follows: 0–20% in 20 min, 20–40% in 30 min, 40–90% in 30 min; 1/10 of the column eluent was split to the electrospray source; ion spray voltage 5 kV; orifice voltage 40 V; scan range m/z 550–1800; scan rate 3 ms/atomic mass unit; resolution > 1 atomic mass unit. The spectra were acquired in centroid mode.

The sequence assignments of a number of CNBr and endoproteinase Glu-C fragments were carried out by analysing the cleavage mixtures, without peptide separations, with MALDI-TOF mass spectrometry. The measurements were performed on a REFLEX™ time-of-flight instrument equipped with a SCOUT™ ion source (Bruker-Franzen Analytik, Bremen, Germany), operating in positive reflectron mode. Ions formed by a pulsed UV laser beam (nitrogen laser, λ = 337 nm) were accelerated at 20 keV. Samples were dissolved in acetonitrile/water (50/50 v/v) to obtain a final concentration of 2.5–5 pmol/μl. Aliquots of 5 μl of analyte solution were added to 5 μl of matrix solution. 0.5 μl of the resulting mixture were deposited on the stainless steel sample holder and allowed to dry at room temperature before introduction into the mass spectrometer. The matrix used was 2,5-dihydroxybenzoic acid, dissolved in acetonitrile/water (50/50, v/v) at a concentration of 1 mg/ml. Mass spectra were obtained averaging 100–200 shots. External calibration was made using the $[M + H^+]^+$ and $[M + 2H^+]^{2+}$ ions of bovine insulin at 5734.56 and 2867.78 Da, respectively.

Table 2
The amino-acid composition of the zinc ion-dependent acid phosphatase

Amino acid	*myo*-IP phosphatase (from sequence data) [a]	Zinc ion-dependent acid phosphatase (± S.E.)
Aspartic acid	25	25.1 ± 0.6
Threonine	17	16.6 ± 0.7
Serine	17	17.5 ± 0.8
Glutamic acid	28	30.3 ± 0.8
Proline	10	n.d.
Glycine	24	23.9 ± 0.4
Alanine	24	23.3 ± 0.5
Valine	23	19.8 ± 0.6
Methionine	10	7.8 ± 0.4
Isoleucine	24	21.5 ± 0.7
Leucine	21	21.3 ± 0.2
Tyrosine	6	6.1 ± 0.2
Phenylalanine	8	8.1 ± 0.3
Lysine	16	15.5 ± 0.4
Histidine	5	5.7 ± 0.3
Arginine	10	10.0 ± 0.3
Cysteine	6	n.d.
Tryptophan	3	n.d.

Protein hydrolysis was carried out in vacuum-sealed vials with 6 M HCl at 110°C for 24 h in triplicate. Serine, threonine and tyrosine data were corrected for loss during hydrolysis. The analyses were performed using a 3A29-Carlo Erba amino-acid analyzer equipped with a computing integrator; amino acids were revealed fluorimetrically with the *o*-phthaldialdehyde reagent.

[a] Taken from [17]. n.d., not determined.

3. Results

3.1. Enzyme purification

Table 1 reports a summary of the purification procedure. At the final step, the enzyme had a specific activity (measured with *p*-nitrophenyl phosphate as substrate and pH 5.5 in the presence of 5 mM $ZnCl_2$) of 66.2 units per mg of protein. This value is about twice higher than that obtained by other authors [7]. The increased PNPP activity at Step 2 compared to that of Step 1 of the purification procedure was probably due to the removal of inhibitors during ammonium sulfate fractionation. The SDS-PAGE analysis of the preparation is shown in Fig. 2: a single band of 31 kDa is present.

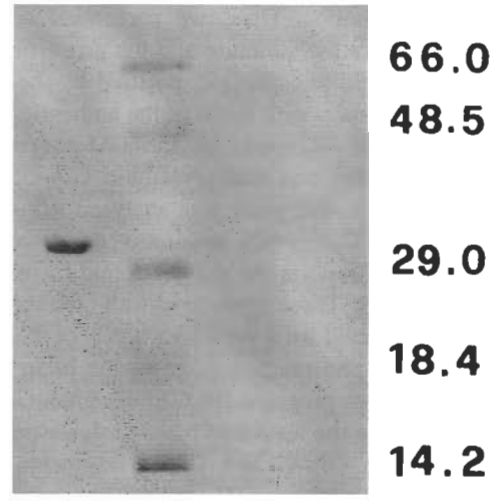

Fig. 2. SDS-PAGE analysis of the purified protein. Lane 1: Zn-dependent acid phosphatase; lane 2: standard proteins. The standard proteins are: bovine α-lactalbumin (14200 daltons), bovine β-lactoglobulin (18400), bovine carbonic anhydrase (29000), porcine fumarase (48500), bovine albumin (66000). Proteins were stained with Coomassie brilliant blue.

3.2. Structural studies

Table 2 shows the amino-acid composition of the carboxymethylated enzyme, whereas Fig. 3 reports the profile of HPLC separation of the fragments obtained by endoproteinase Glu-C digestion. Four peaks, named sp32, sp38, sp42, and sp48 in the HPLC chromatogram, have been sequenced. Table 3 summarises the results. The four peptide sequences were compared with the protein sequences contained in the EMBL Data Bank using the QGSEARCH program (PC/GENE software, IntelliGenetics). All four sequenced peptides revealed 100% amino-acid sequence identity to the corresponding sequences contained in the *myo*-inositol 1-phosphatase. This is one of the key enzymes of the receptor-stimulated inositol phospholipid metabolism. It has been considered the target of Li^+ action in the treatment of humans affected by manic-depressive disease [13,14]. The findings till now obtained induced us to consider the hypothesis that a single protein possesses both Zn^{2+}-dependent acid phosphatase and *myo*-inositol

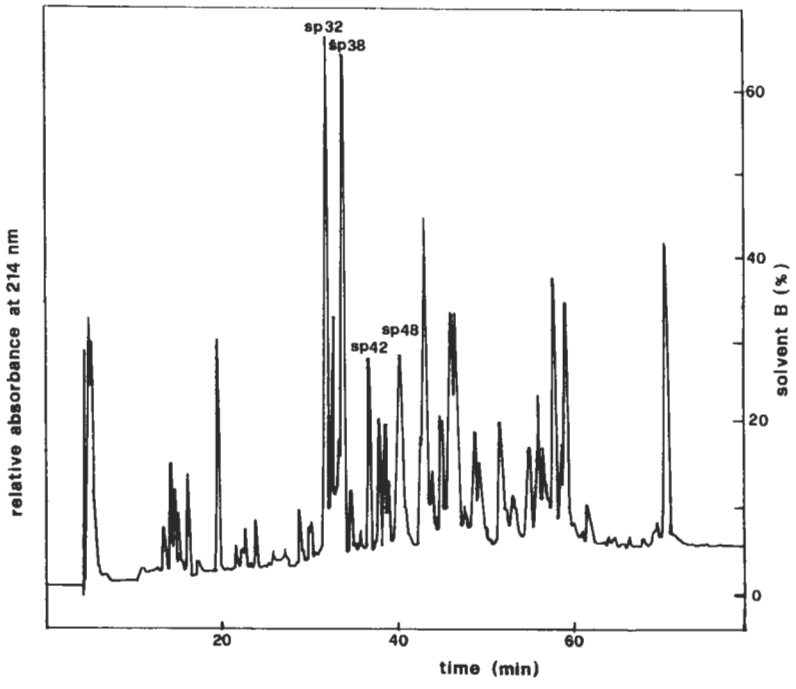

Fig. 3. Reverse-phase HPLC separation of endoproteinase Glu-C peptides obtained from Zn^{2+}-dependent acid phosphatase. Column: peptide and protein C18, 4.6 × 250 mm, 5 μm. Solvent A, 10 mM TFA in water; solvent B, 10 mM TFA in acetonitrile. Flow rate, 0.8 ml/min. (————) absorbance. The elution gradient was as follows: 0–20% solvent B in 30 min; 20–30% solvent B in 20 min; 30–50% solvent B in 25 min; 50–60% solvent B in 10 min.

1-phosphatase activities. Thus, we performed additional analyses to compare the structure and the properties of the Zn^{2+}-dependent acid phosphatase, purified by the method described in this paper, with those of the authentic *myo*-inositol-1-phosphatase. Aliquots of the CM-enzyme were digested with trypsin and endoproteinase Glu-C, respectively. The tryptic hydrolysate was analysed using a continuous flow HPLC/ES-MS apparatus as described in Section 2. Table 3 reports the masses found for a number of tryptic fragments. These agree very well with the masses of fragments predicted for tryptic hydrolysis of the authentic *myo*-inositol 1-phosphatase from bovine brain [15], by using the CLEAVAGE program (PCGENE, IntelliGenetics). Table 3 reports also the results of mass-analyses performed on endoproteinase Glu-C and CNBr fragments with a MALDI-TOF/MS apparatus. These analyses were directly carried out on the non-purified mixtures of peptides obtained by the protein cleavages described above, since this apparatus is able to give the mass values of molecular mixtures, without the need to separate the compounds included in a mixture. It can be seen that several peptides have masses that correspond to those predicted by the CLEAVAGE program set for endoproteinase Glu-C and CNBr cleavage sites, respectively. With the exception of the amino-terminal fragment (from the residue 1 to residue 9), we obtained fragments representative of the entire sequence of the *myo*-inositol 1-phosphatase.

3.3. Kinetic properties of the Zn^{2+}-dependent acid phosphatase

In the absence of divalent metal ions, the enzyme does not catalyse the hydrolysis of *p*-nitrophenyl phosphate at pH 5.5. Fujimoto et al. [7] demonstrated that, among divalent metal ions, Zn^{2+} is the stronger activator. The kinetic parameters, K_m and V_{max}, relative to three aromatic substrates (i.e., *p*-nitrophenyl phosphate, phenyl phosphate and L-phosphotyrosine) were measured in the presence of Zn^{2+} ion at pH 5.5 and 37°C, while those relative to *myo*-inositol 1-phosphate were measured in the presence of Mg^{2+} ion at pH 8.0 and 37°C. The non-linear fittings in the Michaelis equation of the initial rate data measured in triplicate at different substrate concentrations were performed with the FIG.P program (Biosoft). Table 4 reports the K_m and V_{max} values. It can be noted that the Zn^{2+}-dependent acid phosphatase activity shows a K_m value for L-phosphotyrosine that is lower than those found for *p*-nitrophenyl phosphate and phenyl phosphate. This may be

Table 3
Correspondence between peptide from the zinc ion-dependent acid phosphatase and *myo*-inositol 1-phosphatase structure [a]

Peptide position [a]	Type of cleavage	Molecular weight		Assignment method
		calculated [a]	found	
10–31	CNBr	2334.6	2335	MALDI-TOF1MS
31–51	EP–GluC	2277.3	2299 *	MALDI-TOF1MS
35–53	CNBr	2017.4	2018	MALDI-TOF1MS
37–49	Trypsin	1332.4	1332.4 ± 0.2	HPLC1ES-MS
62–78	Trypsin	1807.9	1806.4 ± 1.1	HPLC1ES-MS
78–118	EP-GluC	4549.3	4550	MALDI–TOF1MS
118–130	CNBr	1561.7	1562	MALDI-TOF1MS
128–152	EP-GluC	2869.2	2869	MALDI-TOF1MS
131–200	CNBr	7677.8	7678	MALDI-TOF1MS
146–156	Trypsin	1297.4	1297 ± 0.0	HPLC1ES–MS
157–167	Trypsin	1161.3	1160.9 ± 0.4	HPLC1ES-MS
181–213	EP-GluC	3520.1	3520	MALDI-TOF1MS
201–214	CNBr	1475.6	1498 *	MALDI-TOF1MS
215–246	CNBr	3212.6	3234 *	MALDI-TOF1MS
231–260	EP-GluC	3075.5	3076	MALDI-TOF1MS
247– 277	CNBr	3566.0	3567	MALDI-TOF1MS
265–273	Trypsin	1109.3	1108.8 ± 0.1	HPLC1ES-MS

Position [a]	Peptide name [b]	Sequence results (automatic Edman degradation)									
52–60	sp42	Lys	-Met	-Leu	-Ile	-Thr	-Ser	-Ile	-Lys	-Glu	
		→	→	→	→	→	→	→	→	→	
61–71	sp38	Lys	-Tyr	-Pro	-Ser	-His	-Ser	-Phe	-Ile	-Gly	-Glu -Glu
		→	→	→	→	→	→	→	→	→	→ →
231–237	sp32	Ala	-Gly	-Gly	-Val	-Leu	-Leu	-Asp			
		→	→	→	→	→	→	→			
266–276	sp48	Ile	-Gln	-Ile	-Ile	-Pro	-Leu	-Gln	-Arg	-Asp	-Asp-Glu
		→	→	→	→	→	→	→	→	→	→ →

[a] From the amino-acid sequence of bovine brain *myo*-inositol 1-phosphatase [17].
[b] See Fig. 2.
* Sodium adduct.

due to the amino and carboxyl groups that are present exclusively in the L-phosphotyrosine and that probably increase the substrate binding. On the other hand, the V_{max} value relative to the Zn^{2+}-dependent enzyme for *p*-nitrophenyl phosphate is about one order of magnitude higher than that found for L-phosphotyrosine. Table 4 reports also the K_m and V_{max} values relative to the Mg^{2+}-dependent *myo*-inositol-1-phosphatase activity of our enzyme preparation. The comparison of these values with those previously determined by Gee et al. [11] with the authentic bovine brain *myo*-inositol 1-phosphatase reveals that our findings are similar to those reported by these authors. In particular, our K_m value is practically the same, while our V_{max} value is about 1.5-fold higher than that found by Gee et al. [11]. We think that this experimental difference in the V_{max} value is justified considering the findings of other authors [16]. In fact, Meek et al. [16], which used a purification procedure different from both those of Gee et al. [11] and our, found different final *myo*-inositol 1-phosphatase specific activity in 8 different preparations. These ranged from 2.9 to 6.7 μmol/min per mg protein at 37°C using β-glycerophosphate as substrate. Thus, we think that the kinetic properties of our enzyme preparation with respect to the *myo*-inositol 1-phosphatase activity are not substantially different from those reported by other laboratories. Furthermore, we observe that the ratio between the Zn^{2+}-dependent acid phosphatase and the Mg^{2+}-dependent *myo*-inositol 1-phosphatase activities measured at different purification steps (Table 1) are quite constant during step [2–7]. The very high ratio between Mg^{2+}-dependent *myo*-inositol 1-phosphatase activity and Zn^{2+}-dependent *p*-nitrophenyl phosphatase activity in the tissue extract is certainly due to additional non-specific phosphatases (such as acid and alkaline phosphatases and other enzymes acting on phosphorylated inositols) present in this particular fraction. These data indicate that the Zn^{2+}-dependent acid phosphatase and the Mg^{2+}-dependent *myo*-inositol-1-phosphatase activities co-purify. We studied also the Mg^{2+}-dependent phosphatase activity on some phosphorylated substrates. The data reported in Table 5 demonstrate that our results are similar to those reported by Gee et al. [11], suggesting that the Mg^{2+}-dependent phosphatase substrate specificity of our enzyme preparation agrees well with that of the authentic *myo*-inositol 1-phosphatase. Table 5 reports also the Li^+ ion inhibition of the Mg^{2+}-dependent *myo*-inositol-1-phosphatase activity of our enzyme preparation. All structural and kinetic data suggest that the same protein possesses both Zn^{2+}-dependent and *myo*-inositol-1-phosphate phosphatase activities.

Table 4
Kinetic parameters

	K_m (mM ± S.E.)	V_{max} (μmol/min per mg protein ± S.E.)
p-Nitrophenyl phosphate [a]	1.00 ± 0.12	95.0 ± 4.0
Phenyl phosphate [a]	0.72 ± 0.03	72.3 ± 2.3
L-Phosphotyrosine [a]	0.45 ± 0.06	11.6 ± 0.5
myo-Inositol 1-phosphate [b]	0.17 ± 0.02	21.2 ± 1.0

[a] Measured at 37°C and pH 5.5 in the presence of 5 mM Zn^{2+}.
[b] Measured at 37°C and pH 8.0 in the presence of 3 mM Mg^{2+}.

Table 5
Substrate specificity of the Mg^{2+}-dependent phosphatase activity and Li^+-inhibition

Substrate	Relative activity (%)
D-*myo*-Inositol 1-phosphate	100
D-*myo*-Inositol 1,4-bis-phosphate	< 0.7
D-*myo*-Inositol 1,4,8-triphosphate	< 1
β-Glycerophosphate	34
2′-AMP	52
2′-GMP	40
D-*myo*-Inositol 1-phosphate + 0.8 mM LiCl	71
D-*myo*-Inositol 1-phosphate + 1 mM LiCl	53
D-*myo*-Inositol 1-phosphate + 5 mM LiCl	17
D-*myo* Inositol 1-phosphate + 10 mM LiCl	12
D-*myo*-Inositol 1-phosphate + 20 mM LiCl	11

Rates with D-*myo*-inositol 1,4-bis-phosphate and D-*myo*-inositol 1,4,5-triphosphate were determined at 0.1 mM substrate concentrations. Rates with D-*myo*-inositol 1-phosphate, β-glycerophosphate, 2′-AMP, and 2′-GMP at 2 mM substrate concentrations. The assays were performed at 37°C in 0.04 M Tris-HCl buffer (pH 8.0) containing 2 mM $MgCl_2$, and the reaction was started by adding catalytic amount of enzyme.

3.4. Thermal stability

In order to achieve additional information, we tested the thermal stability of both activities. This test was performed as follows: the enzyme (50 μg), dissolved in 25 mM Tris-HCl buffer (pH 7.0) containing 2 mM 2-mercaptoethanol and 1 mM EDTA, was incubated at 88°C in a screw-cap vial. At increasing times, aliquots were withdrawn and both Zn^{2+}-dependent acid phosphatase and *myo*-inositol-1-phosphatase activities were assayed. Fig. 4 reports the results; it can be seen that the time-dependent loss of both activities was quite similar, suggesting that the same protein catalyses the hydrolysis of both substrates.

3.5. Other features of the enzyme preparation

We studied the effect of pH on both activities; Fig. 5 (A and B) shows the results. In the presence of Mg^{2+} ions, the enzyme shows a pH-optimum in the range 6.5–8.0 for *myo*-inositol-1-phosphatase activity. Also Mg^{2+}-dependent *p*-nitrophenyl phosphatase activity increased to pH 8 and then remained quite constant. On the other hand, both pH-optima shifted to a more acidic zone in the presence of Zn^{2+} ions: with *p*-nitrophenyl phosphate as substrate, the pH-optimum was around 5.5, whereas the pH-optimum with *myo*-inositol 1-phosphate as substrate was around 6.7. It can be noted that the Zn^{2+}-dependent *p*-nitrophenyl

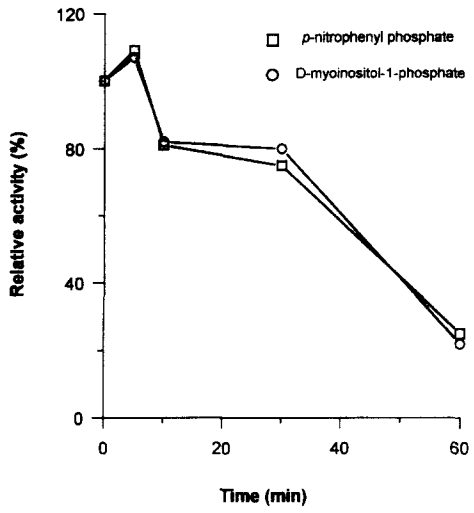

Fig. 4. Thermal stability of Zn^{2+}-dependent acid phosphatase and Mg^{2+}-*myo*-inositol 1-phosphatase activities. The enzyme preparation was incubated at 88°C, and the activities were tested at the indicated times.

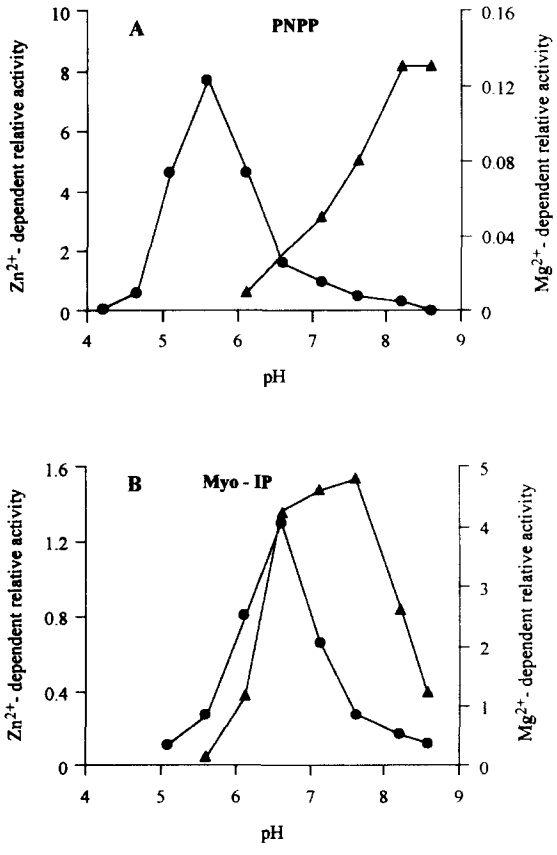

Fig. 5. pH optima of the *p*-nitrophenyl phosphatase (A) and *myo*-inositol 1-phosphatase (B) in the presence of 5 mM Zn^{2+} and 2 mM Mg^{2+} ions. The symbols are as follows: (●) Zn^{2+}-dependent, and (▲) Mg^{2+}-dependent activities. The buffers used were: pH 4.2–7.1, 25 mM sodium 3,3-dimethylglutarate; pH 7.6–8.6, 50 mM Tris-HCl. The substrate concentrations were 4 mM *p*-nitrophenyl phosphate, and 0.1 mM D-*myo*-inositol 1-phosphate.

phosphatase specific activity is higher than that of the Mg^{2+}-dependent *myo*-inositol 1-phosphatase (see Table 1). These data indicate that the pH value changes the enzyme substrate and ion requirement specificity.

4. Discussion

The Zn^{2+}-dependent acid phosphatase was prepared as a pure protein. About 2 mg of enzyme, starting from 2 kg of bovine brain were obtained. At pH 5.5, the zinc ion is an essential activator, since the enzyme shows no activity in the absence of this ion. Also other metal ions are able to replace zinc ion as activator, but their activation ability is lower if compared to that of the Zn^{2+} ion. The enzyme is eluted from the Superdex 200 column at a volume that indicate a molecular weight of about 60 000, whereas SDS-PAGE analysis gives a molecular weight of about 31 000. This suggests that this enzyme is a dimer composed by two subunits of identical molecular weights. A number of structural analyses, which include the determination of the molecular mass of CNBr, trypsin and endoproteinase Glu-C fragments as well as the determination of the amino-acid sequences of four endoproteinase Glu-C peptides, reveal that the Zn^{2+}-dependent acid phosphatase activity is an intrinsic property of a previously described enzyme, i.e. *myo*-inositol-1-phosphatase. In fact, we also demonstrated that, in the presence of Mg^{2+} ions, the enzyme efficiently catalyses the hydrolysis of *myo*-inositol 1-phosphate, and that the Li^{+} ion inhibits this activity, as expected. The molecular features, such as the dimeric nature and the similarity of the apparent molecular weights of the monomers and of the dimer, as well as the substrate specificity of our preparation with respect to a number of substrates previously tested with the authentic *myo*-inositol 1-phosphatase from bovine brain [11], together with the similar thermal sensitivity of both activities, all support the hypothesis that an unique protein possesses both Zn^{2+}-dependent acid phosphatase and Mg^{2+}-dependent *myo*-inositol 1-phosphatase activities.

Finally, we underline that the protein we purified shows higher Zn^{2+}-dependent *p*-nitrophenyl phosphatase activity (in slightly acidic medium) than Mg^{2+}-dependent *myo*-inositol 1-phosphatase activity (in neutral or slightly alkaline media), suggesting that the enzyme acts in vivo also as an aromatic Zn^{2+}-dependent acid phosphatase. Since low M_r aromatic aryl phosphates are not present in cells, the possible in vivo target of the Zn^{2+}-enzyme activity is the phosphotyrosine contained in proteins.

We do not exclude that the two different activities in the same protein may work in different cell compartment and that they are regulated by pH or metal ion species concentrations. Fraústo da Silva and Williams [8] proposed that the zinc stores found in vesicles of particular brain structures are involved in zinc-dependent signalling processes. These vesicles contain millimolar zinc ion concen-

trations, suggesting that brain contains special zinc pumps (unknown to date) that concentrate this ion. These authors highlighted also the similarity of some chemical properties that both calcium and zinc posses, suggesting the idea that the zinc ion, like calcium, participates in particular biological signalling processes.

Acknowledgements

We thank Dr. Roberta Seraglia from C.N.R. Research Area, Padova, for MALDI-TOF MS analyses. This work was supported by grants from Italian C.N.R. and Ministero dell' Università e della Ricerca Scientifica e Tecnologica.

References

[1] Vincent, J.B., Crowder, M.W. and Averill, B.A. (1992) Trends Biochem. Sci. 17, 115–110.
[2] Stone, R.L. and Dixon, J.E. (1994) J. Biol. Chem. 269, 31323–31326.
[3] Hollander, P.V. (1971) in The Enzymes (Boyer, P.D., ed.), Vol. 4, pp. 449–498, Academic Press, New York.
[4] Campbell, H.D. and Zerner, B. (1973) Biochem. Biophys. Res. Commun. 54, 1498–1503.
[5] Kawabe, H., Sugiura, Y., Terauchi, M. and Tanaka, H. (1984) Biochim. Biophys. Acta 784, 81–89.
[6] Hayman, A.R., Warburton, M.J., Pringle, A.S., Coles, B. and Chambers, T.J. (1989) Biochem. J. 261, 601–609.
[7] Fujimoto, S., Gotoh, H., Ohbayashi, T., Yazaki, H. and Ohara, A. (1993) Biol. Pharm. Bull. 16, 745–750.
[8] Fraústo da Silva, J.J.R. and Williams, R.J.P. (1991) in The Biological Chemistry of the Elements (Fraústo da Silva, J.J.R., and Williams, R.J.P., eds.), pp. 299–318, Clarendon Press, Oxford.
[9] Laemmli, U.K. (1970) Nature 227, 680–685.
[10] Baykov, A.A., Evtushenko, O.A. and Avaeva, S.M. (1988) Anal. Biochem. 171, 266–270.
[11] Gee, N.S., Ragan, C.I., Watling, K.J., Aspley, S., Jackson, R.G., Reid, G.G., Gani, D. and Shute, J.K. (1988) Biochem. J. 249, 883–889.
[12] Manao, G., Pazzagli, L., Cirri, P., Caselli, A., Camici, G., Cappugi, G., Saeed, A. and Ramponi G. (1992) J. Protein Chem. 11, 333–345.
[13] Hallcher, L.M. and Sherman, W.R. (1980) J. Biol. Chem. 255, 10897–10901.
[14] Sherman, W.R., Leavitt, A.L., Honcher, M.P., Hallcher, L.M. and Phillips, B.E. (1981) J. Neurochem. 36, 1947–1951.
[15] Diehl, R.E., Whiting, P., Potter, J., Jee, N., Ragan, C.I., Linemayer, D., Schoepfer, R., Bennett, C. and Dixon, R.A.F. (1990) J. Biol. Chem. 265, 5946–5949.
[16] Meek, J.L., Rice, T.J. and Anton, E. (1988) Biochem. Biophys. Res. Commun. 156, 143–148.
[17] Diehl, R.E., Whiting, P., Potter, J., Gee, N., Ragan, C.I., Linemeyer, D., Schoepfer, R., Bennett, C. and Dixon, R.A.F. (1990) J. Biol. Chem. 265, 5946–5949.